JOURNAL OF MATERIALS SCIENCE 26 (1991) 5725–5732

Electron diffraction study of superlattices and orientation variants in $Ca_3SrAl_6SO_{16}$

Y. G. WANG, H. Q. YE, K. H. KUO, X. J. FENG*, G. L. LIAO*, S. Z. LONG*
Laboratory of Atomic Imaging of Solids, Institute of Metal Research, Academia Sinica, Shenyang 110015, People's Republic of China

Samples having the nominal composition of $Ca_3SrAl_6SO_{16}$ were sintered at 1380 °C and analysed by electron diffraction. The frequent appearances of forbidden and satellite reflections in this compound imply the presence of a number of basal and nonbasal superlattices so that the microstructure of this cement clinker was characterized by various superstructures including one-, two- and even three-dimensional superstructures along the ⟨0 0 1⟩, ⟨1 1 0⟩, ⟨1 1 2⟩, ⟨1 1 4⟩ or ⟨2 2 1⟩, ⟨0 1 3⟩ and ⟨1 2 3⟩ directions with repeat periods of two or three times of that of basic one, respectively, and intergrowth of these. Various domain structures with 90°, 120° and 48.2°, etc., orientation relationships were also detected in these superstructures and the total number of these orientation variants related to the symmetry elements lost in the process of phase transformation, can be predicted according to the conclusions of Van Tendeloo and Amerlinckx, or they are equal to the number of those unique planes in the matrix.

1. Introduction

Calcium aluminosulphate, $Ca_4Al_6SO_{16}$ (usually abbreviated to C_4A_3S) with unit cell parameter $a = 0.919$ nm, has a similar arrangement of atoms to ultramarine, a naturally occurring mineral [1]. The X-ray structural determination of C_4A_3S single crystal showed that there are two sets of 8*c* positions, namely Ca_I and Ca_{II} as shown in Fig. 1, occupied by the calcium atoms with different occupations, and the average ratio of occupations on them is 3:1, i.e. Ca_I occupies 3/4 of the calcium atom sites while Ca_{II} occupies 1/4 sites [2]. Thus the calcium atoms can move freely along the channels formed in the direction of body diagonals of the unit cell to some extent, so that a number of superstructures could be introduced to change or invert the occupation of calciums at the two sets of positions. Recently we have investigated the microstructures of C_4A_3S by electron diffraction and high-resolution electron microscopy. The various superstructures and some domain structures resulting from the ordering of calcium cations have been revealed, and structural models of them have been suggested based upon the characteristic arrangement of part occupation of the calcium atoms at these two sets of positions [3, 4]. The structure of $Ca_3SrAl_6SO_{16}$ has a very close relationship to C_4A_3S and therefore it can be reasonably predicted that in this compound these two sets of 8*c* position of calcium should be shared by calcium and stronite disorderly, i.e. keeping the same occupations on these sites as that in C_4A_3S [5]. The superstructure originating from the ordering of atoms, i.e. movement of some of the atoms, whilst others remain at the same positions, resulted in phase transformation as has already been reported in many alloys, and the number of orientation variants as well as translation variants possibly caused by such cases, can also be calculated from the ratio of the order of point groups of the matrix to that of the precipitate [6, 7].

In the present paper we describe the results of an electron diffraction investigation on a cement com-

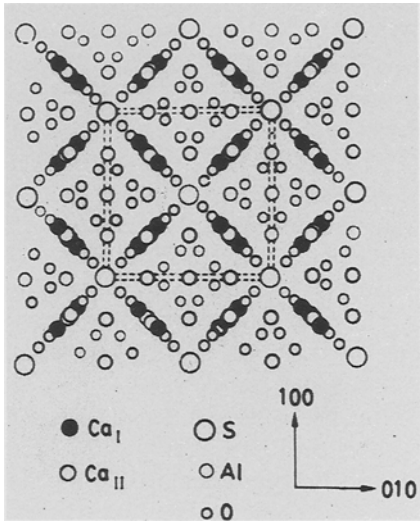

Figure 1 The [0 0 $\bar{1}$] projection of C_4A_3S, Ca_I and Ca_{II} are occupied 3/4 and 1/4 of the calcium sites, respectively, whereas they would be disorderly replaced by calcium and strontium with the same occupations in $Ca_3SrAl_6SO_{16}$.

* Also at Wuhan University of Technology, 14 Luoshi Road, Wuhan 430070, People's Republic of China

0022–2461/91 $03.00 + .12

pound with the composition $Ca_3SrAl_6SO_{16}$. In this cement clinker, some new basal and nonbasal superlattices and orientation variants of these superlattices have been determined unambiguously by selected-area electron diffraction, in addition to those detected previously in C_4A_3S.

2. Experimental procedure

In order to understand the effect of different elements on the microstructure of cement compounds, the cement clinkers under study were prepared by mixing the raw materials in the proportion $2CaO:SrO:3Al_2O_3:CaSO_4$ and pressing the uniformly mixed powders in a cylindrical mould at about 150 MPa. The resulting compact pieces ($\sim$ 20 mm diameter and 10 mm thick) were fired in a platinum container in a platinum–rhodium-wound alumina muffle furnace. No special steps were taken to control the furnace atmosphere because evidence has been presented showing reduction conditions are unlikely to be present in the heating process [8]. The final sintering was at 1380 °C for 8 h. The samples were air quenched after withdrawal from the furnace and examined by X-ray powder diffraction. The results showed the characteristic diffraction features to be nearly the same as those of C_4A_3S and thus the structure of this cement could be thought to be same as that described by Healsted and Moore [1] and Feng *et al.* [2]. The preparations were a slightly yellowish white and brittle. Samples suitable for investigation by electron microscopy were made by grinding them into thin fragments of about 100–1000 nm long in an agate mortar, and then were made into suspensions in absolute alcohol by a supersonic vibration in order to disperse these thin pieces as uniformly as possible in the alcohol. A drop of the suspension was put on a copper grid coated with a holey carbon film and the specimen was examined with a JEM-200CX electron microscope; composition analysis was carried out in a Philips-400T electron microscope equipped with an EDAX 9100 X-ray energy dispersive spectrometer and the standard thin-film correction software supplied by the maker was used.

For observation, various crystals with $\langle 0\,0\,1\rangle$, $\langle 1\,1\,0\rangle$, $\langle 1\,1\,1\rangle$ and $\langle 1\,2\,0\rangle$ orientations were chosen so that the diffraction patterns always included one or two fundamental cell axes and $\langle 1\,1\,0\rangle$ or $\langle 2\,1\,1\rangle$ directions, which make it easy to identify the superstructures as well as orientation variants along these directions. However, some crystallites with different orientations, for instance $\langle 3\,1\,1\rangle$ instead of $\langle 1\,1\,0\rangle$, were also chosen in order to examine some orientation variants. A low beam current density was also used in the observation because $Ca_3SrAl_6SO_{16}$ is also sensitive to the electron beam damage on irradiation.

3. Results and discussion

3.1. Basal superlattice reflections

It is known that because $Ca_3SrAl_6SO_{16}$ has the same arrangement of atoms as C_4A_3S, its structure could, therefore, be well established by putting calcium and strontium in place of calcium at the two sets of 8*c* positions in C_4A_3S. The ordering distribution of calcium or strontium atoms along different planes would cause the superstructures already demonstrated by us [3]. Fig. 2a–d show the [0 0 1] selected electron diffraction patterns of $Ca_3SrAl_6SO_{16}$, where Fig. 2a shows the diffraction pattern of the matrix, and the others show the various superstructures along the $\langle 1\,1\,0\rangle$ directions; Fig. 2b and d are the one- and two-dimensional superstructures, whereas Fig. 2c shows the 90° orientation domains between the one-dimensional superstructure already described [3]. Fig. 3a–d are diffraction patterns obtained with the electron beam parallel to the $[1\,1\,\bar{1}]$ direction of $Ca_3SrAl_6SO_{16}$, the superlattice reflections along one,

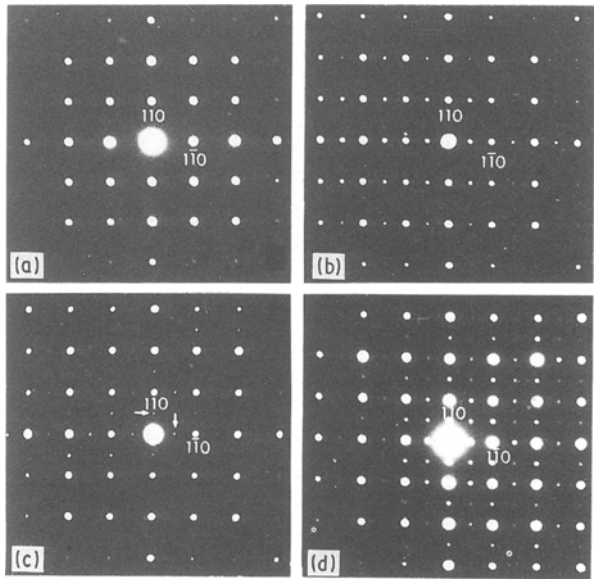

Figure 2 The [0 0 1] electron diffraction patterns of $Ca_3SrAl_6SO_{16}$ showing (a) the fundamental structure, (b) the one-dimensional superlattice, (c) 90° orientation variants of the $2d_{\bar{1}\,1\,0}$ superstructure and (d) the two-dimensional superlattice.

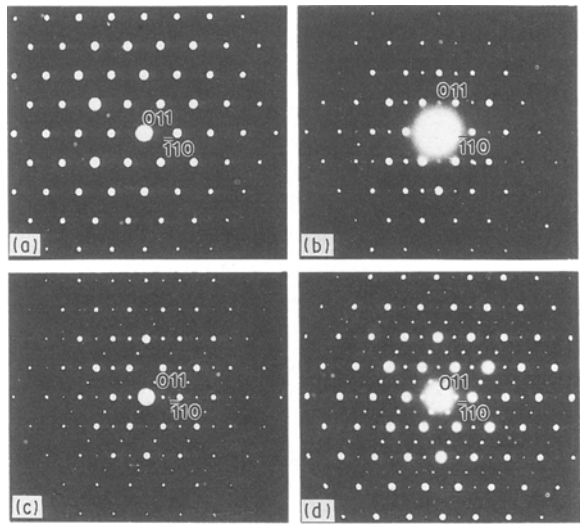

Figure 3 The $[1\,1\,\bar{1}]$ electron diffraction patterns of $Ca_3SrAl_6SO_{16}$ displaying (a) the basic structure, (b) the one-dimensional superlattice, (c) 120° orientation variants and (d) the three-dimensional superlattice.

two and three $\langle 1\,1\,0\rangle$ directions are shown very clearly in Fig. 3b–d, respectively. In fact they correspond to the one-dimensional superstructure, 120° orientation domain and possibly the three-dimensional superstructure in turn. These superstructure and domain structures were earlier reported by us, and the structural models as well as the good match between the simulated images and the observed ones of these superstructures has also been shown for the orderly inverse occupation of calcium atoms on those two sets of positions along the $\langle 1\,1\,0\rangle$ directions. These basal superlattice reflections are all present along the $\langle 1\,1\,0\rangle$ directions in Figs 2 and 3, so that they are the same as the one-, two- and three-dimensional superlattices and 90° and 120° domains determined in C_4A_3S.

In addition to those ordering structures already reported, there is also a new basal superlattice found in $Ca_3SrAl_6SO_{16}$. Fig. 4a–d show electron diffraction patterns with the electron beam parallel to the [1 1 0] direction of $Ca_3SrAl_6SO_{16}$. In addition to the diffraction patterns from the matrix and the $[\bar{1}\,1\,0]$ superlattice exhibited in Fig. 4a and b, forbidden reflections such as 0 0 1 can also be seen in Fig. 4c. Therefore, the superstructure possibly has a period of twice that of the fundamental unit cell and we call it the $2c$ superstructure. Both the superlattice reflections along the $[\bar{1}\,1\,0]$ direction and such forbidden reflections are all present in Fig. 4d, implying their intergrowth and this also shows the ordering arrangement of Ca^{2+} and/or Sr^{2+} cations along the [0 0 1] and $[\bar{1}\,1\,0]$ directions, respectively, in local areas at random in the sample. Fig. 5 shows the suggested structural model of this $2c$ superstructure caused by the ordering inverse occupation of calcium and strontium cations along the [0 0 1] axis so that this superlattice with unit cell parameters $a = 0.919$ nm, $c = 1.838$ nm, $z = 4$ and possible space group $I\bar{4}\,m\,2$, could actually introduce the phase transformation from the cubic to tetragonal.

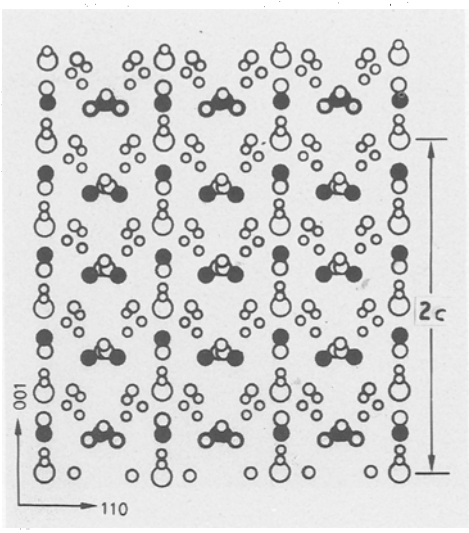

Figure 5 Schematic diagram of the $2c$ superstructure caused by the inverse ordering of cations, where the meanings of the different symbols are as in Fig. 1.

3.2. Nonbasal superlattices and intergrowth of them

Nonbasal superlattices can also be introduced by the ordering of the structure with a long period formed perpendicular to some nonbasal planes in a crystal and have already been found in many materials and minerals [9, 10]. Fig. 6 shows an electron diffraction pattern in the same direction as in Fig. 4. Besides the superlattice reflections already found in Fig. 4b there are also some satellite reflections appearing along the $[1\,\bar{1}\,4]$ or $[2\,\bar{2}\,\bar{1}]$ directions and this suggests that a superlattice with repeat periods of $3d_{1\,\bar{1}\,4}$ and $3d_{2\,\bar{2}\,\bar{1}}$ may be produced in $Ca_3SrAl_6SO_{16}$. In other words, Fig. 6 shows the intergrowth of basal and nonbasal superstructures and it can be predicted reasonably that such a nonbasal superstructure may also be caused by the orderly inverse occupation of calcium and strontium cations on the two sets or the ordering of these two cations with repeat periods of three times of that of the fundamental structure perpendicular to

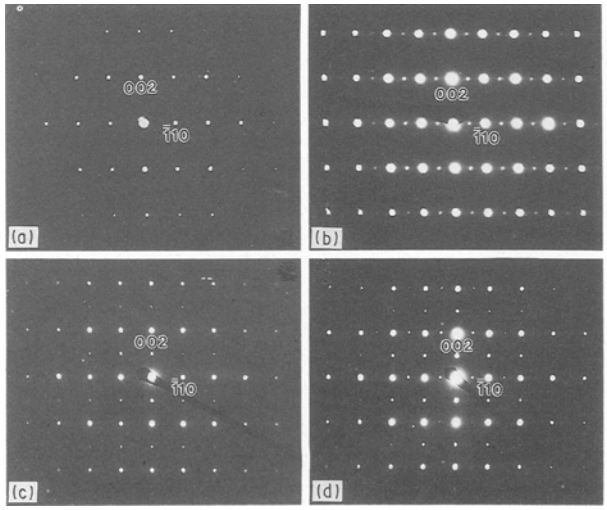

Figure 4 The [1 1 0] electron diffraction patterns of $Ca_3SrAl_6SO_{16}$ illustrating (a) the fundamental structure, (b) $2d_{\bar{1}\,1\,0}$ superlattice, (c) $2c$ superlattice and (d) intergrowth of these two kinds of superlattices.

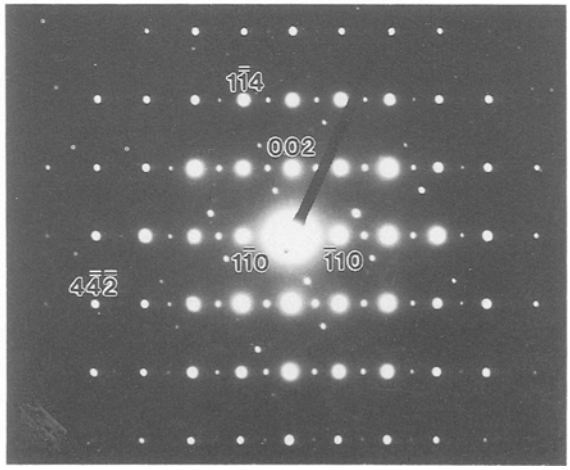

Figure 6 The electron diffraction pattern with the beam parallel to the [1 1 0] direction of $Ca_3SrAl_6SO_{16}$ showing the intergrowth of the $2d_{\bar{1}\,1\,0}$ superlattice and the nonbasal superlattice with periods of $3d_{1\,\bar{1}\,4}$ and $3d_{2\,\bar{2}\,\bar{1}}$.

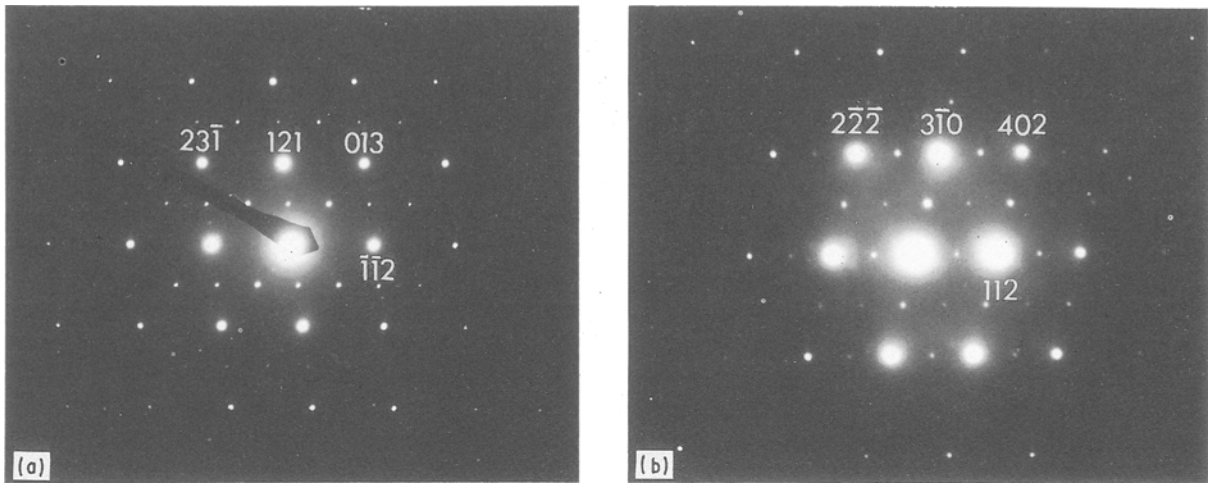

Figure 7 (a) The [$\bar{5}$ 3 $\bar{1}$] diffraction pattern showing the intergrowth of (1 2 1) and (0 1 3) or (2 3 $\bar{1}$) superlattices, and (b) the intergrowth of (1 1 2), (3 $\bar{1}$ 0) and (2 0 1) or (1 $\bar{1}$ $\bar{1}$) superlattices, with the beam parallel to [1 3 $\bar{2}$].

the $d_{1\,\bar{1}\,4}$ and $d_{2\,\bar{2}\,\bar{1}}$ planes, because the qualitative analysis of composition on these fields of X-ray energy dispersive spectrometry shows no obvious difference in aspect of ratio of the elements compared to that of the matrix. The characteristic feature of this new superlattice is coincident with the two-dimensional case. In such a case, the unit cell parameters could be chosen as $a' = 1.3$ nm, $b' = 1.93$ nm, $c' = 2.76$ nm, where they equal the lengths of the [1 1 0], 1/2[1 $\bar{1}$ 4] and [2 $\bar{2}$ $\bar{1}$] vectors, respectively, and their orientation relationships between this nonbasal superstructure and the matrix are $a' \parallel [1\,1\,0]$, $b' \parallel [2\,\bar{2}\,\bar{1}]$, $c' \parallel [1\,\bar{1}\,4]$. The phase transformation from the cubic to orthorhombic or monoclinic possibly may be created as well.

In addition to the co-existence of the basal superstructures and nonbasal superlattices, the intergrowth between nonbasal superlattices is also frequently found in the sample. For example, Fig. 7a shows the intergrowth of superlattices with periods twice that of the basic cell along [1 2 1] and [2 3 $\bar{1}$] or [0 1 3] directions, whereas Fig. 7b shows the intergrowth of (1 1 2), (3 $\bar{1}$ 0) and (2 0 1) or (1 1 1) superlattices. It should be pointed out that these superstructures can also be introduced by an alternate ordering distribution of calcium and strontium cations along those directions in the matrix even if there is only one set of 8*c* positions available for these two kinds of cations in $Ca_3SrAl_6SO_{16}$ cement compound. This is distinct from the C_4A_3S case.

3.3. Orientation variants

According to the conclusions of Amerlinckx and coworkers [6, 7] the number of orientation variants related by the lost symmetry elements in the process of phase transformation from matrix to precipitate, for example in the case of the $\langle 1\,1\,0 \rangle$ superstructures, has already been calculated and observed in C_4A_3S by the present authors [4]. In the same way, the number of orientation variants in the case of $\{0\,0\,1\}$ superlattices can also be simply calculated from the theory of point groups. During the phase transformation from cubic to tetragonal, only the three-fold symmetry of the basic cell is destroyed so that the factor of the order of the point group of the fundamental unit cell divided by that of the superstructure is equal to 3, i.e. there will only be three orientation variants possibly produced. In other words there are three $\langle 0\,0\,1 \rangle$ directions in the matrix on the whole, and they are perpendicular to each other. Therefore only the 90° orientation variants may be constructed for this basal superstructure.

Fig. 8 shows the [0 0 $\bar{1}$] electron diffraction pattern of $Ca_3SrAl_6SO_{16}$, in which the forbidden reflections along the [0 $\bar{1}$ 0] and [1 0 0] axes can be seen, indicating that the 90° orientation domain structure would be invariably present. In a similar way, the number of orientation variants of the $\{h\,h\,l\}$ superlattice could also be calculated. In such a case this number is equal to the number of unique orientations of $\{h\,h\,l\}$ planes, because the matrix is a noncentral symmetrical crystal and thus the inversion boundary as well as inversion variants, i.e. 180° anti-orientation variants, cannot be formed. In a cubic cell there are 24 $\{h\,h\,l\}$ planes in total, but the unique orientations (excluding the opposite orientations) are only half this number (12). The

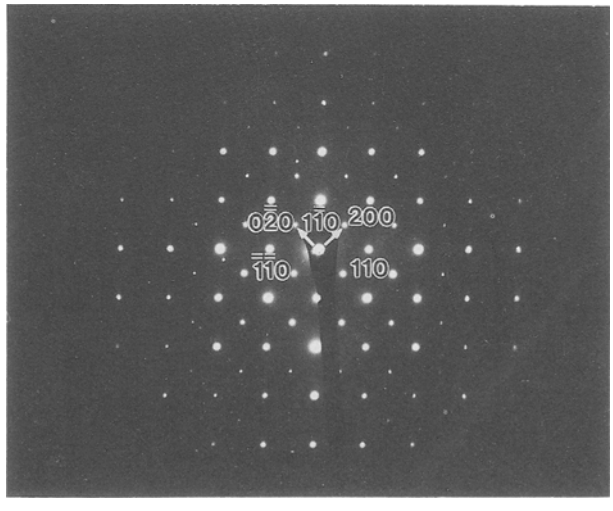

Figure 8 The [0 0 $\bar{1}$] electron diffraction patterns showing 90° orientation variants of the 2*c* superstructure.

superlattices may be introduced along these directions with equal possibility. Therefore, the number of orientation variants in this case is 12. The five angles between these directions can be assumed, and it suggests that there will be in total five kinds of orientation domain structure possibly caused for such ordered phases. As an example, the results given in Table I were computed based upon the $\{1\,1\,2\}$ superlattices. They are 35.6°, 48.2°, 60°, 70.5° and 80.4° in turn, in which there are some variants related by the symmetry elements lost in the process of phase transformation, for example 60° and 70.5° orientation variants are related by three-fold symmetry and mirror reflection, respectively. The others, however, do not connect with these lost symmetry elements. Thus those orientation variants should be observed along different directions. The 35.6° orientation variants can only be viewed along the $\langle\bar{3}\,1\,1\rangle$ directions and the result is shown in Fig. 9, which is obtained with the electron beam parallel to the $[3\,\bar{1}\,1]$ direction. In this figure the superlattice reflections along both the $[\bar{1}\,\bar{1}\,2]$ and $[1\,2\,1]$ directions are present. Therefore, it may indeed be reliable evidence for the presence of $\{1\,1\,2\}$ 35.6° orientation variants, as analysed in Table I. Because $[\bar{3}\,1\,1]$ is a general direction, i.e. there is no symmetry element present along this orientation, the orientation angle of these two variants is not limited by those symmetrical operations in the fundamental structure.

The order of the point group of the $\{1\,1\,2\}$ superstructure could also be calculated from the order of the point group of the matrix divided by the number of orientation variants of the precipitate, and the result will be 2, because it has in total 12 orientation variants, i.e. there are two symmetrical operations remaining. Furthermore, the phase transformation from cubic to monoclinic may be produced in the presence of such a superstructure. Variants with an orientation angle of 48.2° are shown in Fig. 10a and the $\langle 1\,1\,2\rangle$ superlattice spots and the forbidden reflection along the $[0\,0\,1]$ direction are all present in Fig. 10b, so that this may imply the intergrowth of these 48.2° orientation variants and the $2c$ superlattice. We assume in Table I that the crystallites with $\langle\bar{5}\,3\,1\rangle$ orientations were selected as proof of the presence of 80.4° orientation variants of the $\{1\,1\,2\}$ superlattices, and the result is shown in Fig. 11, where the two variants separated at 80.4° are seen in Fig. 11a and Fig. 11b demonstrates the intergrowth of these variants and the $(2\,3\,1)$ or $(0\,1\,\bar{3})$ superlattices.

Generally, there are 12 unique $\{h\,k\,0\}$ planes in the cubic cell so that it can be predicted that the number of orientation variants is 12 for $\{h\,k\,0\}$ superlattices, and as a result the orientation angles between them could also be estimated. On the other hand, it can be stated that there will be six kinds of domain structure probably caused in this case. In a similar way to the

TABLE I The possible orientation variants introduced in the $\{1\,1\,2\}$ superlattices

Possible orientation of superlattices	Orientation angle (deg)	Direction of observation
$[1\,1\,2]$, $[1\,2\,1]$	35.6	$\langle\bar{3}\,1\,1\rangle$
$[1\,1\,2]$, $[\bar{1}\,1\,2]$	48.2	$\langle 0\,2\,\bar{1}\rangle$
$[1\,1\,2]$, $[\bar{1}\,2\,1]$	60	$\langle 1\,1\,\bar{1}\rangle$
$[1\,1\,2]$, $[\bar{1}\,\bar{1}\,2]$	70.5	$\langle 1\,\bar{1}\,0\rangle$
$[1\,1\,2]$, $[1\,2\,\bar{1}]$	80.4	$\langle\bar{5}\,3\,1\rangle$

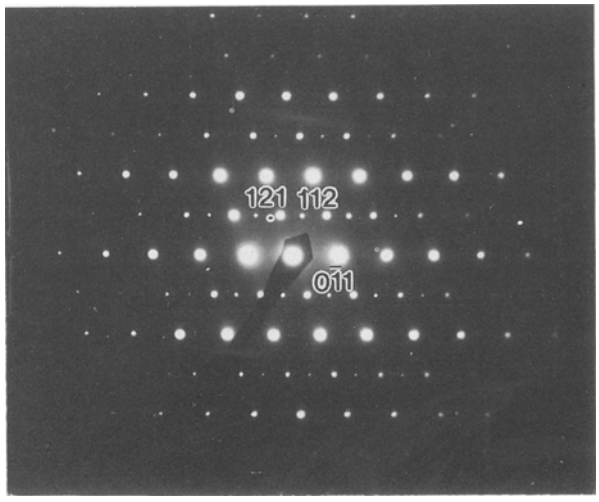

Figure 9 The diffraction pattern showing the 35.6° orientation variants of the $\{1\,1\,2\}$ superlattices, with the beam projected along $[\bar{3}\,1\,1]$.

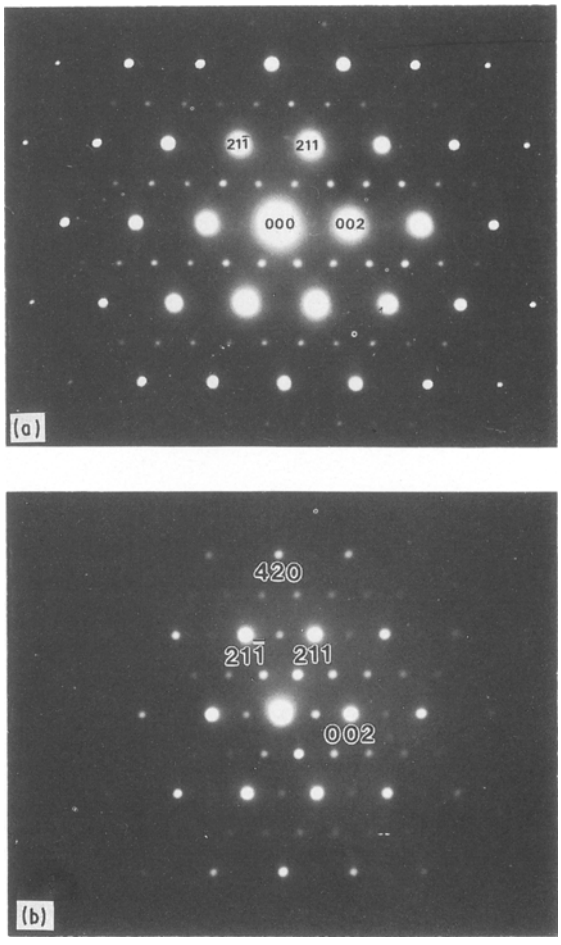

Figure 10 The $[\bar{1}\,2\,0]$ diffraction patterns showing the 48.2° orientation variants of (a) the $\{1\,1\,2\}$ superlattice and (b) the intergrowth of these orientation variants and the $2c$ superlattice.

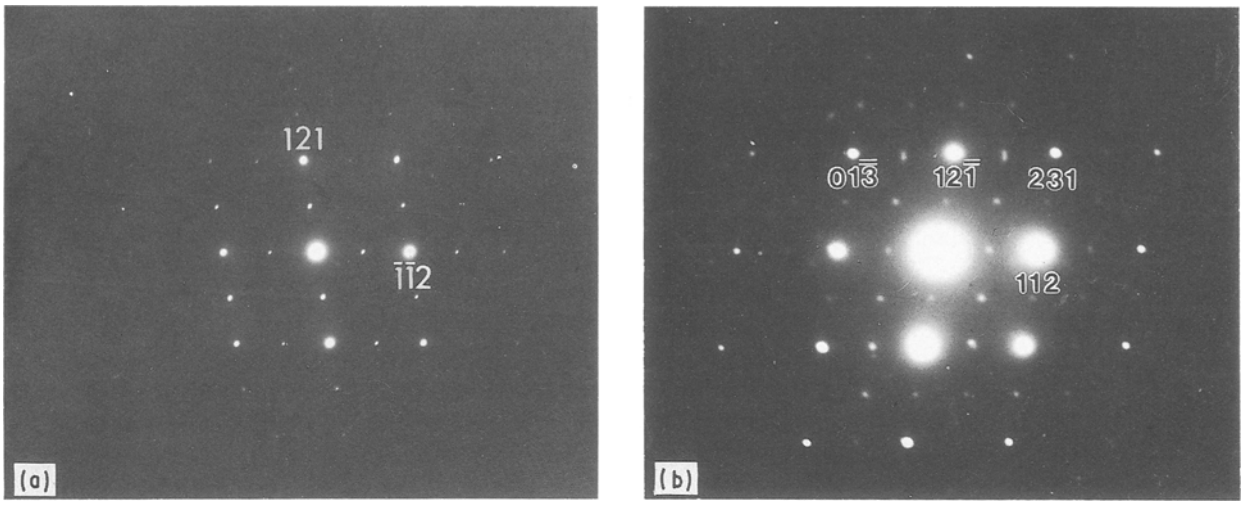

Figure 11 The diffraction patterns with the beam parallel to the $[\bar{5}\,3\,\bar{1}]$ and $[\bar{5}\,3\,1]$ directions, respectively, showing (a) the 80.4° orientation variants of the $\{1\,1\,2\}$ superlattices and (b) the intergrowth of such variants and the $(2\,3\,1)$ or $(0\,1\,\bar{3})$ superlattices.

TABLE II The orientation variants possibly introduced in the $\{0\,1\,3\}$ superlattices

Possible orientation of superlattices	Orientation angle (deg)	Direction of observation
$[0\,1\,3]$, $[1\,0\,3]$	25.8	$\langle 3\,3\,\bar{1}\rangle$
$[0\,1\,3]$, $[0\,\bar{1}\,3]$	36.9	$\langle 1\,0\,0\rangle$
$[0\,1\,3]$, $[0\,3\,1]$	53.1	$\langle \bar{1}\,0\,0\rangle$
$[0\,1\,3]$, $[3\,0\,1]$	72.5	$\langle 1\,9\,\bar{3}\rangle$
$[0\,1\,3]$, $[3\,1\,0]$	84.3	$\langle \bar{1}\,3\,\bar{1}\rangle$
$[0\,1\,3]$, $[0\,3\,\bar{1}]$	90	$\langle \bar{1}\,0\,0\rangle$

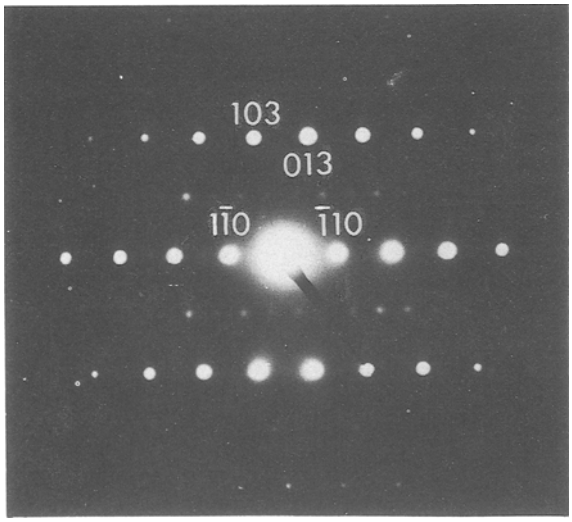

Figure 12 The $[3\,3\,\bar{1}]$ diffraction pattern illustrating the 25.8° orientation variants of the $\{0\,1\,3\}$ superlattices.

TABLE III Possible orientation variants introduced in the $\{1\,2\,3\}$ superlattices

Possible orientation of superlattices	Orientation angle (deg)	Direction of observation
$[1\,2\,3]$, $[1\,3\,2]$	21.8	$\langle \bar{5}\,1\,1\rangle$
$[1\,2\,3]$, $[\bar{1}\,2\,3]$	31	$\langle 0\,\bar{3}\,2\rangle$
$[1\,2\,3]$, $[2\,3\,1]$	38.2	$\langle \bar{7}\,5\,\bar{1}\rangle$
$[1\,2\,3]$, $[3\,2\,1]$	44.4	$\langle \bar{1}\,2\,\bar{1}\rangle$
$[1\,2\,3]$, $[2\,\bar{1}\,3]$	50	$\langle 9\,3\,\bar{5}\rangle$
$[1\,2\,3]$, $[\bar{2}\,3\,1]$	60	$\langle \bar{1}\,\bar{1}\,1\rangle$
$[1\,2\,3]$, $[1\,\bar{2}\,3]$	64.6	$\langle 3\,0\,\bar{1}\rangle$
$[1\,2\,3]$, $[\bar{2}\,\bar{1}\,3]$	69.1	$\langle 3\,\bar{3}\,1\rangle$
$[1\,2\,3]$, $[\bar{1}\,\bar{2}\,3]$	73.4	$\langle 2\,\bar{1}\,0\rangle$
$[1\,2\,3]$, $[3\,\bar{2}\,1]$	81.8	$\langle 1\,1\,\bar{1}\rangle$
$[1\,2\,3]$, $[1\,3\,\bar{2}]$	85.9	$\langle \bar{1}\,\bar{3}\,5\,1\rangle$

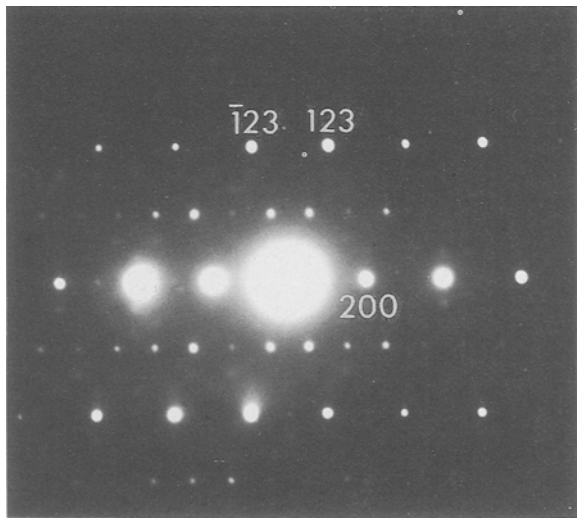

Figure 13 The diffraction pattern showing the 31° orientation variants of the $\{1\,2\,3\}$ superlattices, with the beam incident along the $[0\,\bar{3}\,2]$ direction.

$2d_{1\,1\,0}$ superstructure, the kinds of orientation variants possibly produced in $\{1\,3\,0\}$ superlattices may also be calculated, and are given in Table II. Fig. 12 shows its 25.8° orientation variants. The order of point groups of this superstructure is still 2 and its unit cell is most probably monoclinic, thus the phase transformation from cubic to monoclinic would also be introduced. For $\{h\,k\,l\}$ superlattices the number of orientation variants will be as large as 24, and 16 kinds of such domain structures may be formed, but in some cases the number of different kinds of domain structure may be less than 16. For example, there are only

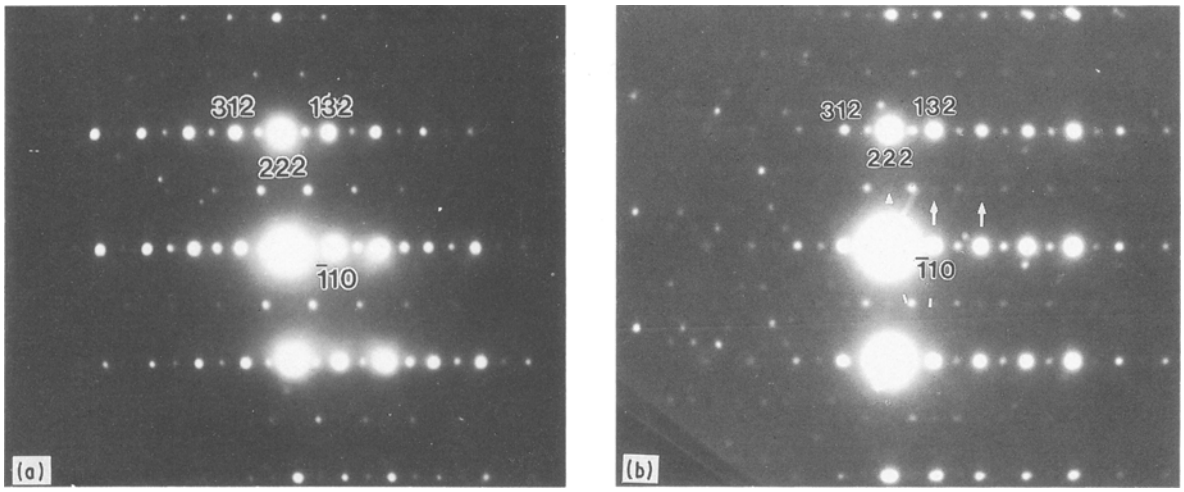

Figure 14 The [1 1 $\bar{2}$] diffraction patterns demonstrating 44.4° orientation variants of (a) $2d_{1\,2\,3}$ superlattices and (b) the coexistence of such variants with $2d_{\bar{1}\,1\,0}$ and $2d_{1\,1\,1}$ superlattices.

TABLE IV The possible superlattices and kinds of orientation variants in $Ca_3SrAl_6SO_{16}$

Superlattices	Symmetry	Order of point group	Number of variants	Kinds of domain
$2d_{0\,0\,1}$	tetragonal	8	3	1
$2d_{1\,1\,0}$	tetragonal	4	6	2
$2d_{1\,1\,1}$	trigonal	6	4	1
$2d_{0\,1\,3}$	monoclinic	2	12	6
$2d_{1\,1\,2}$	monoclinic	2	12	5
$2d_{1\,2\,3}$	triclinic	1	24	11

11 kinds of domain structure in the {1 2 3} superstructures as shown in Table III. Fig. 13 shows the 31° orientation variants, and the 44.4° domains are illustrated in Fig. 14a; moreover the forbidden reflection of 1 1 1 and a satellite spot between the two basic spots of $\bar{1}$ 1 0 appearing in Fig. 14b indicate the intergrowth of these domain variants with the ($\bar{1}$ 1 0) and (1 1 1) superlattices. The order of point groups of the {1 2 3} superlattice could be predicted as above, being equal to 1, i.e. only one symmetry element, one-fold symmetry (identity), remaining, so that the phase transformation from cubic to triclinic may be introduced.

4. Conclusion

The evidence from electron diffraction study shows clearly that the fine structure of $Ca_3SrAl_6SO_{16}$ is similar to C_4A_3S. The one- to three-dimensional superstructures resulting from the ordering of cations could also be found in this analogous cement compound. In addition to those superstructures already found in C_4A_3S, there are also some basal and non-basal superlattices, as well as newly discovered orientation variants. These superstructures and domain variants are all summarized in Table IV, although some of them have not yet been confirmed. Therefore, the microstructure of this cement clinker is also characterized by the intergrowth of various superstructures and orientation variants. So many superlattices and domains strongly imply that they may practically relate to the ordering of different kinds of cations along the ⟨1 0 0⟩, ⟨1 1 0⟩, ⟨1 1 1⟩, ⟨1 1 2⟩, ⟨0 1 3⟩ and ⟨1 2 3⟩, etc., directions in the basic structure, respectively. Such ordered superstructures also suggest that certain cations or groups might probably be errant in the structure, having no fixed position but being able to move or oscillate within the framework, i.e. cations could move from place to place, although the magnitude may be very small, along the channels in the direction of the body diagonals of the fundamental unit cell, as concluded by Jaeger in his study of ultramarine [11], or at least some of such constituents could jump from one position to the next, while the others have fixed positions, as predicted by Taylor in analogous zeolites [12].

Acknowledgement

The authors thank Dr W. M. Bian, Laboratory of Electron Microscopy of the Northeast University of Technology, for permitting use of the Philips-400T electron microscope.

References

1. P. E. HEALSTED and A. E. MOORE, *J. Appl. Chem.* **12** (1962) 413.
2. X. J. FENG, G. L. LIAO and S. Z. LONG, *J. Chinese Silicate Soc.* **18** (1990).
3. Y. G. WANG, H. Q. YE, *et al. J. Mater. Sci.* **26** (1991).
4. Y. G. WANG, H. Q. YE, *et al. ibid.* **25** (1990).
5. G. L. LIAO, Dissertation, Wuhan University of Technology (1988).

6. G. VAN TENDELOO and S. AMERLINCKX, *Acta Crystallogr.* **A30** (1974) 431.
7. S. AMERLINCKX and R. VAN LUNDY, "Electron microscopy in mineralogy", (Springer-Verlag, New York, 1976) pp. 206–50.
8. T. A. RAGOZINA, *Zh. Prikl. Khim.* **30** (1957) 1682.
9. L. PIERCE and P. R. BUSECK, *Amer. Mineral.* **63** (1978) 1.
10. H. BOHM, *Amer. Mineral.* **68** (1983) 11.
11. F. M. JAEGER, "Georger Fisher Baker Memorial lectures", Vol. 7, Part III (Cornell University, 1930).
12. W. H. TAYLOR, *Z. Krist.* **74** (1930) 1.

Received 15 March
and accepted 20 December 1990